


Assessment of immunoglobulin heavy chain, immunoglobulin light chain, and T-cell receptor clonality testing in the diagnosis of feline lymphoid neoplasia

Emily D. Rout  | Robert C. Burnett | Janna A. Yoshimoto | Paul R. Avery |
Anne C. Avery

Department of Microbiology, Immunology and Pathology, College of Veterinary Medicine and Biomedical Sciences, Colorado State University, Fort Collins, Colorado

Correspondence

A C Avery, Department of Microbiology, Immunology and Pathology, College of Veterinary Medicine and Biomedical Sciences, Colorado State University, 200 West Lake Street, Fort Collins, CO 80523.
Email: anne.avery@colostate.edu

Abstract

Background: Differentiation between neoplastic and reactive lymphocytic proliferations can be challenging in cats. PCR for antigen receptor rearrangements (PARR) testing is a useful diagnostic tool to assess clonality of a lymphoid population. Previous feline PARR studies evaluated clonality of complete immunoglobulin heavy chain V-D-J (IGH-VDJ) and T-cell receptor gamma (TRG) gene rearrangements.

Objectives: We aimed to evaluate the sensitivity and specificity of feline PARR primers targeting complete IGH-VDJ and TRG rearrangements, as well as incomplete IGH-DJ, kappa deleting element (Kde), and immunoglobulin lambda light chain (IGL) gene rearrangements in defined feline neoplasms and nonneoplastic controls.

Methods: Fluorescently labeled PCR primers were designed to amplify complete IGH-VDJ, incomplete IGH-DJ, Kde, IGL, and TRG gene rearrangements in two multiplexed PCR reactions, and PCR products were analyzed by fragment analysis. Fresh tissue samples from 12 flow cytometrically confirmed B-cell lymphomas, 26 cytologically confirmed gastric and renal lymphomas of presumed B-cell origin, 30 flow cytometrically confirmed T-cell leukemias, and 11 negative control cats were tested.

Results: Using four immunoglobulin primer sets (IGH-VDJ, IGH-DJ, Kde, and IGL), clonal immunoglobulin rearrangements were detected in 87% (33/38) of the presumed B-cell neoplasms. The IGH-VDJ reaction alone only detected clonality in 50% (19/38) of these cases. TRG rearrangements were clonal in 97% (29/30) of the T-cell leukemia cases. All negative control samples had polyclonal immunoglobulin and TRG rearrangements.

Conclusions: The PARR assay developed in this study is useful for assessing clonality in feline lymphoid neoplasms. Clonality assessment of incomplete IGH-DJ, Kde, and IGL rearrangements helped identify clonal B-cell neoplasms not detected with complete IGH-VDJ PARR alone.

KEYWORDS

antigen receptor rearrangement, lymphoma, T-cell receptor gamma

1 | INTRODUCTION

Lymphoma is a common malignancy in cats, and in recent years, feline gastrointestinal lymphoma has become one of the most prevalent forms.^{1,2} Diagnosis of feline lymphoma can be challenging with cytology³⁻⁵ and histology,⁵⁻⁸ given the propensity for cats to develop small cell lymphoma. Feline lymphomas can also arise from a chronic inflammatory population, so that neoplastic lymphocytes are intermixed with reactive lymphocytes, further complicating diagnoses.^{5,9} A PCR-based assay to determine clonality of antigen receptor gene rearrangements can be a useful tool to differentiate neoplastic from reactive lymphoid populations.^{5,6,9,10}

The PCR for antigen receptor rearrangements (PARR) assay evaluates the length of rearranged antigen receptor genes. Antigen receptors are generated by the rearrangement of different genes of the immunoglobulin (IG) and T-cell receptor (TCR) loci. In IG heavy chain (IGH) rearrangements, diversity (D) and joining (J) genes are rearranged first, followed by rearrangement of a variable (V) gene with the D-J rearrangement. In IG kappa (IGK), IG lambda (IGL), and TCR gamma (TRG) loci, V genes rearrange directly with J genes. In the TRG locus, the V genes and J genes are grouped with a constant (C) gene into multiple V-J-C cassettes. During gene rearrangements, nucleotides are subtracted and added at the junctions between genes. This junctional region forms the third complementarity determining region (CDR3), and its length is unique to individual lymphocytes. In the PARR assay, a region of the antigen receptor gene rearrangement that includes the CDR3 is amplified by PCR and products are separated based on length.^{10,11} A reactive lymphoid population will reveal a polyclonal population of different-sized antigen receptors, and a neoplastic population should reveal a clonal antigen receptor of one size. A single clonal cell population might have a rearrangement on both alleles of the antigen receptor locus, which generates a biclonal pattern. In T-cell neoplasms, multiple cassettes can rearrange, resulting in multiple clonal TRG products, which should not be interpreted as an oligoclonal result.¹²

Previous studies have characterized the feline IGH and TRG loci and developed primers to detect clonality of these antigen receptors.^{9,13-24} V genes in the feline IGH locus (IGHV genes) are grouped into three subgroups based on nucleotide sequence similarities,^{14,15,24} with the majority of rearrangements using genes homologous to the human IGHV3 subgroup.^{15,24} Previous studies have designed PARR primers to target the most common IGHV3 subgroups,^{13,19,21} as well as the less common IGHV1 subgroups.^{13,19} IGHJ primer pools were designed to cover the two most commonly rearranged IGHJ genes, and degenerate primers were developed to account for the variability in the remaining IGHJ genes.^{13,19,21} The TRG locus was targeted for PARR because these genes rearrange early in T-cell development, and the rearrangement persists in T cells expressing an alpha-beta TCR.²⁵ The feline TRG locus is reported to contain three subgroups of TRGV genes, which include functional TRGV genes and TRGV pseudogenes. There are three subgroups of TRGJ genes.^{9,16-18}

The reported sensitivity for detecting a clonal TRG by PCR in T-cell neoplasms has been relatively high, with 5/7 studies reporting sensitivities $\geq 79\%$.^{9,18,20,22,26-28} The sensitivity for detecting a clonal IGH receptor among feline B-cell neoplasms has been historically lower, with sensitivity values ranging from 34% to 89%.^{13,19,21-23,26,28} One difficulty in detecting B-cell neoplasms is that the IGH receptor can undergo somatic hypermutation, altering nucleotides at primer sites, which compromises primer binding. Another challenge in assessing the diagnostic accuracy of the feline PARR assay in finding a gold standard to classify patients accurately. Most studies use histology and immunohistochemistry as a gold standard, but histology has limitations in both correctly detecting feline lymphoma⁵ and identifying lineage, especially in challenging cases with mixed B cells and T cells.²⁶

To improve the sensitivity of detecting feline B-cell neoplasms, we expanded the PARR assay to assess clonality of additional types of IG rearrangements. In addition to complete IGH-VDJ gene rearrangements, the IGH locus can also yield incomplete rearrangements between IGHD and IGHJ genes that fail to combine with an IGHV gene (termed IGH-DJ rearrangements), which could be assessed for clonality. Additionally, in human medicine, targeting the IG light chain rearrangements for clonality testing has improved detection of B-cell neoplasms that have undergone somatic hypermutation.¹¹ During human B-cell development, IGK genes are rearranged first, but if a functional IGK product is not produced, the IGK allele is inactivated through rearrangement of the kappa deleting element (Kde), and subsequently IGL genes are rearranged. Cats preferentially express lambda light chains, suggesting many feline B cells have undergone Kde recombination to inactivate the IGK locus.^{15,29} Therefore, assessing clonality in Kde rearrangements and IGL rearrangements could improve the sensitivity of PARR in B-cell neoplasms compared with IGH PARR alone.

The purpose of this study was to evaluate the diagnostic accuracy of our laboratory's PARR assay in detecting feline B-cell and T-cell neoplasms. Additionally, we investigated the added value of detecting clonality in IGH-DJ, Kde, and IGL rearrangements, as compared with traditional IGH-VDJ rearrangements, for detection of feline B-cell lymphomas.

2 | MATERIALS AND METHODS

2.1 | Study design

PCR primers were designed for the amplification of IG and TRG gene rearrangements to assess B-cell and T-cell clonality (Figure 1 and Table 1). For the IG locus, four primer sets were developed: (a) IGH-VDJ primers target complete IGH rearrangements from the V region to the J region; (b) IGH-DJ primers target incomplete IGH rearrangements from the D region to the J region; (c) IG kappa deleting element (Kde); (d) IG lambda light chain (IGL) rearrangements from the V region to the J region. For the T-cell receptor locus, primer sets were developed to target TRG rearrangements from the V region to the J region.

PARR was performed on feline B-cell neoplasms, T-cell neoplasms, and negative control samples. Assays were developed for use on fresh tissue and air-dried cytologic preparations. Because histologic specimens were rarely collected and there are limitations of the histologic assessment of feline small cell lymphomas, we chose several strategies to enhance our ability to detect true feline B-cell and T-cell neoplasms. First, we collected samples that had a definitive diagnosis of B-cell lymphoma by flow cytometry, and a cytology report consistent with lymphoma, irrespective of the anatomic location. Second, we identified gastric and renal samples with a definitive diagnosis of lymphoma by cytology. These sites were chosen because previous reports indicated that the vast majority of feline gastric and renal lymphomas are of B-cell lineage.^{22,30-32} For T-cell neoplasms, we tested T-cell leukemia cases with a moderate to marked lymphocytosis, using flow cytometry as a gold standard to determine lineage. Fresh lymphoid tissue and blood were collected from negative control cats without lymphoproliferative diseases.

2.2 | Flow cytometry

Flow cytometry was performed on a subset of B-cell cases, all T-cell cases, and all negative control cases. The remaining B-cell cases were cytologically confirmed gastric and renal lymphoma cases that were collected retrospectively, so flow cytometry was not available. Flow cytometric cell preparation, staining, and analytic methods are provided in the Supporting information.

2.3 | Antigen receptor loci characterization and primer design

2.3.1 | IGH locus

For all loci, gene sequence analysis and primer design were performed with Geneious software (<https://www.geneious.com>). To amplify complete IGH-VDJ rearrangements, we designed PCR forward primers to amplify IGHV3 and IGHV1 subgroup genes and reverse primers to amplify IGHJ genes. cDNA sequences of feline IGHV3 and IGHV1 clones from Mochizuki et al¹⁹ were aligned to identify regions with high sequence homology. One IGHV1 subgroup primer (IGHV-f1) and one IGHV3 subgroup primer (IGHV-f2) were designed in the third framework (FR3) region. We identified five IGHJ genes in the germline DNA sequence from cat chromosome B3 (Felis catus 9.0 assembly, GenBank Assembly ID GCA_000181335.4), and all of the IGHJ sequences from recently published IGH mRNA transcripts¹⁵ appeared to map to these five IGHJ genes. Four IGHJ reverse primers were designed to amplify all five IGHJ genes.

To amplify incomplete IGH-DJ rearrangements, we first identified candidate feline germline IGHD genes. We used human and canine IGHD genes to design motifs containing nucleotides spanning the nonamer and heptamer recombination sites on either side of IGHD genes. Germline DNA sequences from the feline chromosome B3 upstream of the IGHJ genes was probed with the IGHD motifs, and 12 feline candidate IGHD genes were identified. A forward

primer was designed for each candidate gene within the upstream intron, and then pools of primers were tested. The primer pool that generated the strongest polyclonal distribution among control samples was selected, which recognizes four of the candidate IGHD genes (IGHD-f1-IGHD-f4 primers). The IGHJ primer pool is similar to the IGH-VDJ reaction, except that one primer was shortened to allow for in-frame triplicate spacing of products.

2.3.2 | TRG locus

TRGV, TRGJ, and TRGC genes within the TRG locus from cat chromosome A2 (NCBI reference ID NC_018724.3, Felis catus 9.0 assembly) were annotated using guidelines established by the international ImMunoGeneTics information system (IMGT) (<http://www.imgt.org>).³³ The feline TRG locus contains six V-J-C cassettes. A prototypical cassette contains two TRGV genes, two TRGJ genes, and one TRGC gene. There are nine TRGV genes belonging to three subgroups and 11 TRGJ genes. TRG gene localization and functionality information were submitted to the IMGT database and are provided in Table S2. For TRG PCR amplification, one forward FR3 primer (TRGV-f2) previously published by Moore et al⁹ amplifies TRGV1 subgroup genes, and a second forward FR3 primer (TRGV-f1) was designed to target the TRGV2 subgroup gene in cassette 5 (TRGV2-3) after Weiss et al¹⁶ reported rearrangements from this cassette. Except for cassette 4, each of the six TRG V-J-C cassettes contains two TRGJ genes. The TRGJ gene proximal to the C gene in a cassette tends to be functional. These similarly oriented TRGJ genes share homology across the cassettes, and a single reverse primer (TRGJ-r1) was designed to anneal this set of TRGJ genes. The TRGJ gene distal to the C gene within a cassette is nonfunctional, and these six TRGJ genes are homologous and targeted by a second reverse primer (TRGJ-r2).

2.3.3 | Kappa deleting element

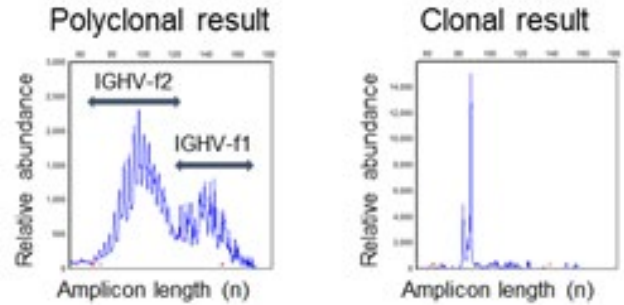
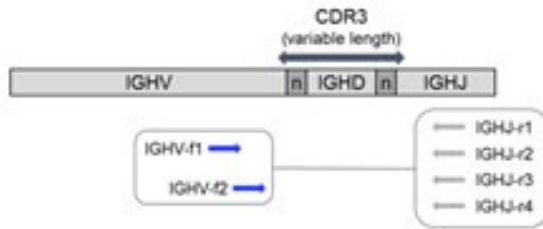
We used human motifs to identify the Kde and the upstream heptamer recombination signal located within the intron between the IGKJ genes and IGKC gene in the feline IGK locus (chromosome A3, Felis catus 9.0 assembly). A forward primer (IGKDE-f) was designed in the IGKJ-IGKC intron 5' to the heptamer, and a reverse primer (IGKDE-r) was designed 3' to the Kde.

2.3.4 | IGL locus

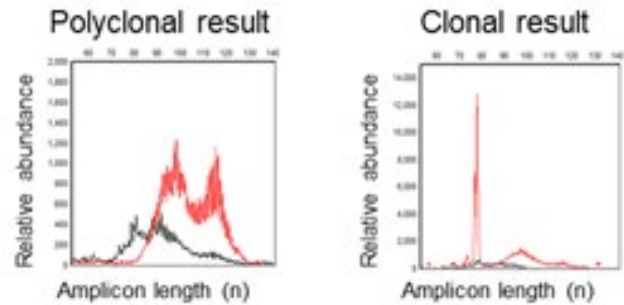
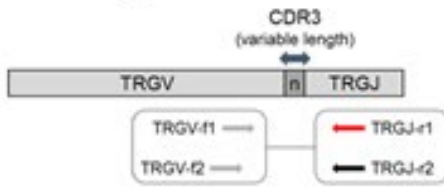
To identify feline IGL genes, a discontinuous MegaBLAST search was performed using human and canine IGLV and IGLJ genes. Seventy-nine IGLV genes belonging to nine subgroups mapped to chromosome D3 (NCBI reference ID NC_018734.3, Felis catus 9.0 assembly). Downstream of these IGLV genes, nine IGLJ genes and nine IGLC genes were arranged in nine J-C clusters, with each IGLC gene preceded by one IGLJ gene. IGL gene localization and functionality information were submitted to the IMGT database and are provided in Table S3. One forward PCR primer (IGLV-f) was designed

PCR reaction 1: IGH-VDJ and TRG rearrangements

A Complete IGH-VDJ rearrangements

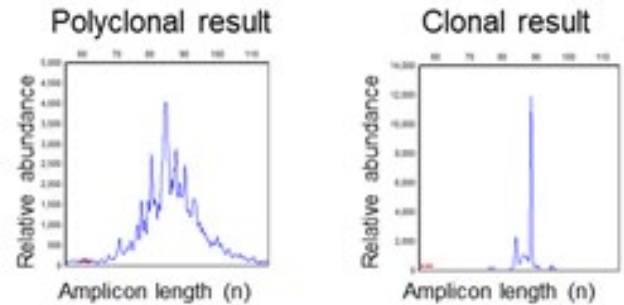
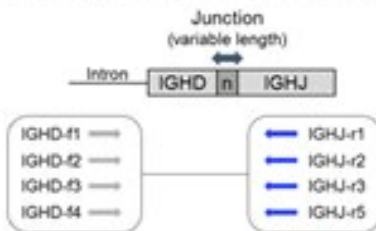


B TRG rearrangements

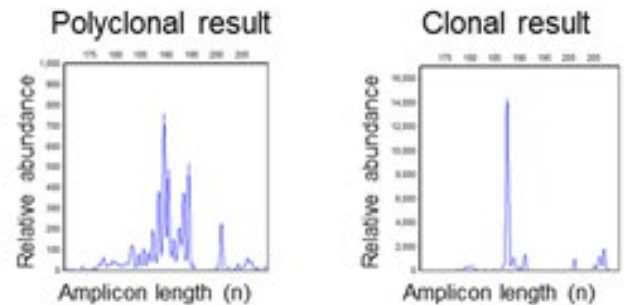
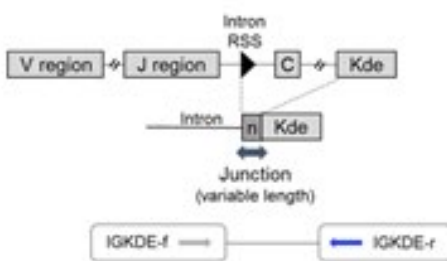


PCR reaction 2: IGH-DJ, Kde and IGL rearrangements

C Incomplete IGH-DJ rearrangements



D Kde rearrangements



E IGL rearrangements

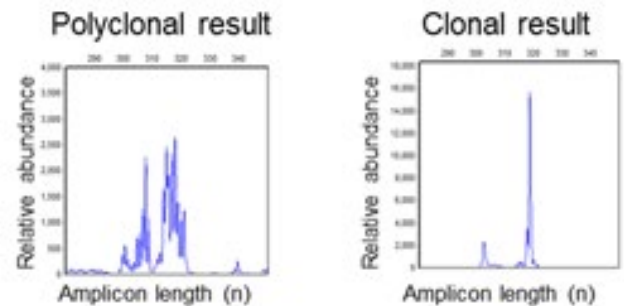
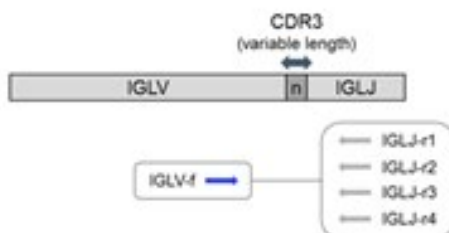


FIGURE 1 Schematic representations of the gene rearrangements, PCR for antigen receptor rearrangements (PARR) primers, and PARR GeneMarker results for complete immunoglobulin heavy chain V-D-J (IGH-VDJ) (A), T-cell receptor gamma (TRG) (B), incomplete immunoglobulin heavy chain D-J (IGH-DJ) (C), kappa deleting element (Kde) (D), and immunoglobulin lambda (IGL) light chain (E) reactions. The variable (V), diversity (D), and joining (J) gene rearrangements are depicted as appropriate for each locus. Nucleotides (n) are added and subtracted at gene junctions, generating a third complementarity determining region (CDR3) of variable length. A, Complete IGH-VDJ gene rearrangement amplification: forward IGHV gene primers, labeled with fluorescein amidite (FAM, blue) dye, bind the framework 3 (FR3) region of IGHV1 subgroup (IGHV-f1) or IGHV3 subgroup (IGHV-f2) genes. Four reverse IGHJ gene primers are unlabeled (IGHJ-r1 – IGHJ-r4 primers). B, TRG rearrangement amplification: unlabeled forward primers bind FR3 of TRGV genes (TRGV-f1 and TRGV-f2), and reverse primers bind TRGJ genes (TRGJ-r1, PET [red]; TRGJ-r2, NED [black]). C, Incomplete IGH-DJ rearrangement amplification: unlabeled forward primers (IGHD-f1 – IGHD-f4 primers) bind intron regions 5' to IGHD genes. FAM-labeled (blue) reverse primers bind IGHJ genes (IGHJ-r1 – IGHJ-r5 primers). D, The immunoglobulin kappa (IGK) locus is inactivated by rearrangement of the Kde into the recombination signal (RSS) within the intron between IGK J and constant (C) genes. The junctional region is targeted with a forward primer (IGKDE-f, unlabeled) 5' to the RSS heptamer and a reverse primer (IGKDE-r, FAM-labeled (blue)). E, IGL rearrangement amplification: a forward FAM-labeled (blue) IGLV-f primer targets IGLV1 subgroup genes, and a pool of unlabeled reverse primers bind the IGLJ genes (IGLJ-r1 – IGLJ-r4 primers). In PCR reaction 2, amplicons for the three loci are different sizes, so that PCR products from IGH-DJ, Kde, and IGL reactions do not overlap on the GeneMarker tracing

TABLE 1 PCR for antigen receptor rearrangements (PARR) primers for the amplification of feline immunoglobulin (IG) and T-cell receptor gamma (TRG) genes

Primer name ^a	Binding site	Fluorescent label	Sequence (5' – 3')	Expected size (nucleotides)
PCR primer combination 1: IGH-VDJ and TRG rearrangements				
IGHV-f1	IGHV1 subgroup	FAM	GACACATCCACAAACACAGCC	110-170
IGHV-f2	IGHV3 subgroup	FAM	AAGACCGAGGACACGGCCACATAY	70-130
IGHJ-r1	IGHJ1/4		AGGASACGGTGACCAGGG	
IGHJ-r2	IGHJ2		GGGAGACGRTGACCTGGG	
IGHJ-r3	IGHJ3		ACACCGTCACCAGGGCTCC	
IGHJ-r4	IGHJ5		TGAGGACACTGTGACTATGGTTC	
TRGV-f1	TRGV2-3		GGATGCTGGTCTGTATTACTGCG	
TRGV-f2 ^b	TRGV1 subgroup		AAGAGCGAYGAGGGMGTGT	
TRGJ-r1	TRGJ	PET	TGACCCTGAGCAGTGTGCCAG	80-125
TRGJ-r2	TRGJ	NED	GTTACGATGASCTTAGTTCCTCTGTC	70-105
PCR primer combination 2: IGH-DJ, Kde and IGL rearrangements				
IGHD-f1	IGHD3		GGGCTTTTTGACGGGGAACCTTC	65-110
IGHD-f2	IGHD4		CCTGGTTATTGTTCATGGGGCATC	
IGHD-f3	IGHD6		CCCCAGCAGCCAAGAGGTTTA	
IGHD-f4	IGHD7		TTGGTGATTTTGTGCAGGCC	
IGHJ-r1	IGHJ1/4	FAM	AGGASACGGTGACCAGGG	
IGHJ-r2	IGHJ2	FAM	GGGAGACGRTGACCTGGG	
IGHJ-r3	IGHJ3	FAM	ACACCGTCACCAGGGCTCC	
IGHJ-r5	IGHJ5	FAM	AGGACACTGTGACTATGGTTC	
IGKDE-f	5'Kde		GTGCGCTAGCCACTAAAGG	
IGKDE-r	3'Kde	FAM	TTCCAGGGGAGAATGAGTC	180-200
IGLV-f	IGLV1 subgroup	FAM	CTGACTCAGCCGGCCTCAGTGTC	300-340
IGLJ-r1	IGLJ1/2/5/7/8		GACGGTCAGATGGGTMCCCTC	
IGLJ-r2	IGLJ4/9		GACGGTCACCTKGGTCCCTC	
IGLJ-r3	IGLJ3		GATGGTCACCCGGTCCCAT	
IGLJ-r4	IGLJ6		GACCGTCAGCCAGGTCCCTC	

IGH-VDJ, complete immunoglobulin heavy (IGH) chain variable (V)-diversity (D)-joining (J) gene rearrangement; IGH-DJ, incomplete immunoglobulin heavy chain diversity (D)-joining (J) gene rearrangement; Kde, kappa deleting element; IGL, immunoglobulin lambda; FAM, fluorescein amidite.

^aPrimer names containing "f" are forward-oriented primers, and those containing "r" are reverse-oriented primers.

^bSource: Primer reported in Moore et al.⁹

TABLE 2 Signalment and sample site information for flow cytometrically confirmed B-cell lymphoma cases and cytologically confirmed gastric and renal lymphoma cases

Case number	Group	Age (years)	Gender	Breed	Site sampled for PARR	Material source for PARR
1	FC-confirmed	15.4	MC	DLH	Spleen	Flow pellet
2	FC-confirmed	13.0	MC	DSH	Lymph node	Flow pellet
3	FC-confirmed	9.0	MC	DSH	Lymph node-mesenteric	Flow pellet
4	FC-confirmed	15.8	FS	DSH	Spleen	Flow pellet
5	FC-confirmed	6.0	FS	DSH	Hepatic	Flow pellet
6	FC-confirmed	6.6	MC	DSH	Renal	Cytology slides
7	FC-confirmed	18.5	FS	DLH	Mass (nasopharyngeal)	Flow pellet
8	FC-confirmed	18.3	MC	DSH	Lymph node-mesenteric	Flow pellet
9	FC-confirmed	15.0	FS	DSH	Intestine	Flow pellet
10	FC-confirmed	16.3	FS	DSH	Renal, intestine (ileum)	Cytology slides
11	FC-confirmed	16.0	MC	DSH	Lymph node	Flow pellet
12	FC-confirmed	16.2	FS	DLH	Lymph node	Flow pellet
13	Cytology-confirmed	16.4	FS	U	Gastric	Cytology slides
14	Cytology-confirmed	8.7	MC	DLH	Renal	Cytology slides
15	Cytology-confirmed	11.0	FS	DSH	Gastric	Cytology slides
16	Cytology-confirmed	15.2	FS	DMH	Renal	Cytology slides
17	Cytology-confirmed	11.0	FS	DSH	Gastric	Cytology slides
18	Cytology-confirmed	16.1	FS	DSH	Gastric	Cytology slides
19	Cytology-confirmed	12.5	U	DSH	Renal	Cytology slides
20	Cytology-confirmed	13.5	FS	MCC	Gastric, lymph node	Cytology slides
21	Cytology-confirmed	12.7	FS	U	Gastric	Cytology slides
22	Cytology-confirmed	2.5	MC	OSH	Renal	Cytology slides
23	Cytology-confirmed	1.8	MC	DSH	Gastric	Cytology slides
24	Cytology-confirmed	U	U	U	Renal	Cytology slides
25	Cytology-confirmed	U	MC	DLH	Gastric	Cytology slides
26	Cytology-confirmed	12.4	FS	SIAM	Gastric	Cytology slides
27	Cytology-confirmed	12.0	MC	MCC	Gastric	Cytology slides
28	Cytology-confirmed	13.8	MC	DSH	Gastric	Cytology slides
29	Cytology-confirmed	15.2	FS	U	Gastric, lymph node	Cytology slides
30	Cytology-confirmed	11.5	MC	DSH	Renal	Cytology slides
31	Cytology-confirmed	8.0	MC	MCC	Gastric, lymph node	Flow pellet & cytology slides
32	Cytology-confirmed	14.3	FS	DSH	Gastric	Cytology slides
33	Cytology-confirmed	14.5	F	DSH	Gastric	Cytology slides
34	Cytology-confirmed	10.4	FS	DLH	Renal, lymph node	Cytology slides
35	Cytology-confirmed	14.0	FS	DSH	Gastric	Cytology slides
36	Cytology-confirmed	9.7	MC	OSH	Renal	Cytology slides
37	Cytology-confirmed	13.1	MC	SIAM	Gastric	Cytology slides
38	Cytology-confirmed	4.6	FS	DSH	Renal, intestine	Cytology slides

Note: Site sampled: when two sites are listed, cellular material from these sites were combined for PARR analysis.

Abbreviations: PARR, PCR for antigen receptor rearrangements; FC, flow cytometry; U, unknown; F, female intact; FS, female spayed; MC, male castrated. Breed abbreviations: DLH, Domestic Longhair; DSH, Domestic Shorthair; DMH, Domestic Medium Hair; MCC, Maine Coon Cat; OSH, Oriental Shorthair; SIAM, Siamese.

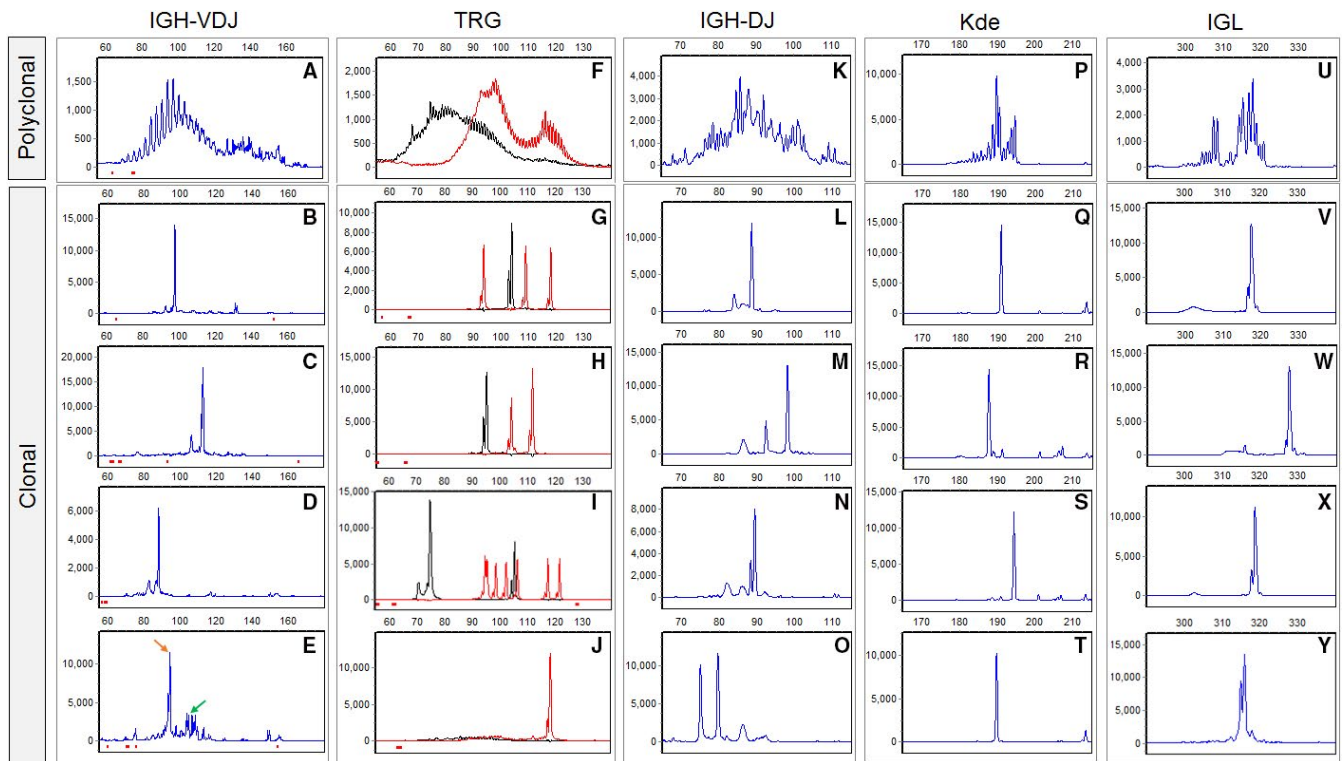


FIGURE 2 PCR for antigen receptor rearrangements (PARR) GeneMarker results for polyclonal and clonal rearrangements from complete immunoglobulin heavy (IGH) chain variable (V)-diversity (D)-joining (J) (IGH-VDJ) (A-E), T-cell receptor gamma (TRG) (F-J), incomplete immunoglobulin heavy chain D-J (IGH-DJ) (K-O), kappa deleting element (Kde) (P-T), and immunoglobulin lambda (IGL) light chain (U-Y) reactions. Polyclonal results are shown in the top panel for each type of rearrangement (A, F, K, P, U). Four different clonal cases are shown for each type of rearrangement to demonstrate the range of results. As depicted in E, a clonal peak (orange arrow) is >3000 in amplitude (vertical axis) and $>3\times$ the height of the polyclonal base (green arrow). For IGH-VDJ rearrangements, clonal products of high amplitude are shown (B, C), as well as a lower amplitude case that is still $3\times$ the base (D), and a higher amplitude case that is slightly $3\times$ the base (E) (height of base: 3,500; height of clonal peak: 11,500). For TRG rearrangements, cases G-I demonstrate clonal peaks with the TRGJ-r1 (red) and TRGJ-r2 (black) primers, while case J has a single clonal rearrangement with the TRGJ-r1 primer. IGH-DJ, Kde, and IGL polyclonal rearrangements (K, P, U) have narrow size distributions with a weaker Gaussian distribution compared with IGH-VDJ (A) and TRG (F). Three cases with a clonal IGH-DJ rearrangement (L-N), and a case with biclonal IGH-DJ rearrangements (O) are shown. Four cases with clonal Kde rearrangements (Q-T), and four cases with clonal IGL rearrangements (V-Y) are shown

to target the major IGLV1 subgroup, and four reverse primers were designed to recognize all IGLJ genes.

2.4 | PCR analysis of IG and TRG rearrangements

For B-cell cases, DNA was isolated from cell pellets or cytologic slide preparations (Table 2). In six cases, two anatomic sites were combined to yield a sample with adequate cellularity (Table 2). DNA was isolated from the peripheral blood or cell pellets for the T-cell leukemia cases and fresh, homogenized lymph node biopsies and peripheral blood samples for the negative control cases. DNA was extracted using a QIAamp DNA Mini Kit (QIAGEN) according to the manufacturer's instructions. For cytologic slide preparations, 200 μL of lysis buffer was pipetted onto the slide surface, the sample was scraped into a microcentrifuge tube (Life Science Products), and the blade was rinsed with 280 μL 1X phosphate buffered saline.

IGH-VDJ and TRG gene rearrangements were amplified in one reaction, and IGH-DJ, Kde, and IGL rearrangements were amplified in a second reaction. Individual primer sets were labeled with

fluorescein amidite (FAM) (Integrated DNA Technologies), PET, or NED fluorescent dyes (Thermo Fisher Scientific), and reactions labeled with the same dye were designed to yield different-sized PCR products so that multiple primer sets could be multiplexed in one amplification reaction (Table 1 and Figure 1). For each sample, approximately 100-500 ng of DNA was amplified with the QIAGEN Multiplex PCR Master Mix kit, which uses HotStarTaq DNA Polymerase, and 200 nmol/L of each primer in a 25 μL reaction volume. The optional Q-Solution provided in the kit was used in the second PCR reaction (for IGH-DJ, Kde, and IGL rearrangements) according to the manufacturer's recommendations. For each reaction, a negative control was included by substituting water for the DNA sample. The cycling conditions were as follows: initial denaturation at 95°C for 15 minutes; then 10 cycles of 94°C for 30 seconds, 64-59°C for 30 seconds (decreasing by 0.5°C every cycle), and 72°C for 1.5 minutes; then 30 cycles of 94°C for 30 seconds, 59°C for 30 seconds, and 72°C for 1.5 minutes; then a final extension of 72°C for 7 minutes. The amplicon length was determined by fragment analysis on an ABI 3130xl system (Applied Biosystems) using

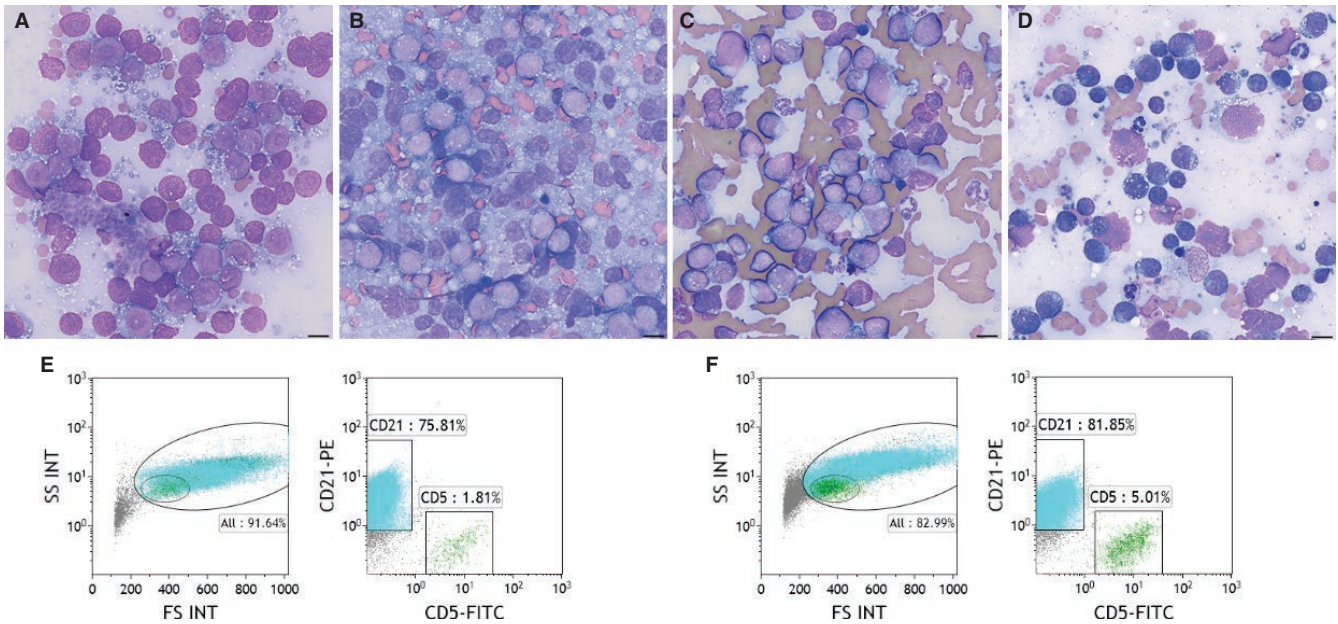


FIGURE 3 Cytologic patterns of gastric (A and B) and renal (C and D) lymphoma in four cats, and flow cytometric immunophenotyping of two cases with B-cell lymphoma (E and F). (A–D) Direct smears of fine-needle aspirates from gastric lesions in two cases (A–B) and renal lesions in two cases (C and D) included in the cohort of feline cases with cytologically confirmed gastric and renal lymphoma, Wright-Giemsa stain, X50 objective. Lymphocytes are predominantly intermediate to large with round nuclei, dispersed to coarse chromatin, variably prominent large round nucleoli, and small amounts of basophilic cytoplasm with punctate vacuoles. Size bar, 10 μ m. (E–F) Flow cytometric immunophenotyping of a hepatic aspirate (E) and a mesenteric lymph node aspirate (F) from two cases included in the cohort of feline cases with flow cytometrically confirmed B-cell lymphoma. For each case, size plots on the left with forward scatter integral linear scale (FS INT) on the horizontal axis and side scatter integral log scale (SS INT) on the vertical axis show small-sized T cells (green) within a small-size gate (delineated by the small grey circle) and intermediate to large-sized B cells (blue). Fluorescence dot plots on the right show that neoplastic B cells (blue) expressing CD21 account for the majority of the leukocyte population. There are small numbers of CD5⁺ T cells (green). Small numbers of neutrophils and monocytes are depicted in grey and express high levels of CD18 (data not shown)

the DS-33 Dye Set (Thermo Fisher Scientific). The PCR product was diluted tenfold, and 1 μ L was added to 14.5 μ L HiDi formamide and 1 μ L GS600LIZ size standard. Data analysis was carried out with GeneMarker software (Soft Genetics).

2.5 | Analysis

Representative polyclonal and clonal results for each PCR reaction are shown in Figure 2. An IGH, Kde, or IGL clonal peak was defined as a tall narrow peak >3000 in amplitude and >3x the height of the base peaks forming the polyclonal background (Figure 2E). A sample with two distinct peaks reaching these criteria was characterized as biclonal. Two peaks that differed in size by a single nucleotide were interpreted as a peak with a “plus A” artifact, resulting from a non-templated A nucleotide added during PCR amplification. If one of these two peaks met diagnostic criteria, the peak was considered clonal. A TRG reaction was considered clonal if one or more peaks met diagnostic clonal criteria. In theory, there could be up to 10 TRG rearrangements, since multiple cassettes can rearrange in a T-cell neoplasm. In practice, the most clonal peaks detected in a T-cell leukemia case were eight. Samples with multiple peaks forming a Gaussian distribution within the expected size range were characterized as polyclonal. IGH-DJ, Kde, and IGL rearrangements have smaller junctional areas compared with IGH-VDJ rearrangements,

and their polyclonal distributions were narrower and less Gaussian in shape compared with the IGH-VDJ assay.

Cases included in this study were determined to have sufficient target DNA based on PARR results. Cases deemed nondiagnostic due to low DNA quantity or quality had low amplitude, nonreproducible oligoclonal peaks with all primers sets. If DNA quantity or quality appeared low based on these criteria, the sample was repeated. The sample was then considered nondiagnostic if oligoclonal peaks were of different lengths, and polyclonal distributions were not detected for any primer set, indicating insufficient target DNA for amplification of both B-cell and T-cell populations.

PARR results were independently and blindly interpreted by the authors (EDR and ACA). Diagnostic sensitivity and specificity were calculated to evaluate the performance of the PARR assay for TRG and IG gene rearrangements in the chosen sample types. In addition, calculations were performed for the IGH-VDJ primers alone, to compare the performance of IGH-VDJ-only PARR with IG PARR including the IGH-DJ, Kde, and IGL primers.

2.6 | Cases

Fifteen cases of flow cytometrically confirmed B-cell lymphoma were collected from January 13, 2017 to September 7, 2018. Tissue

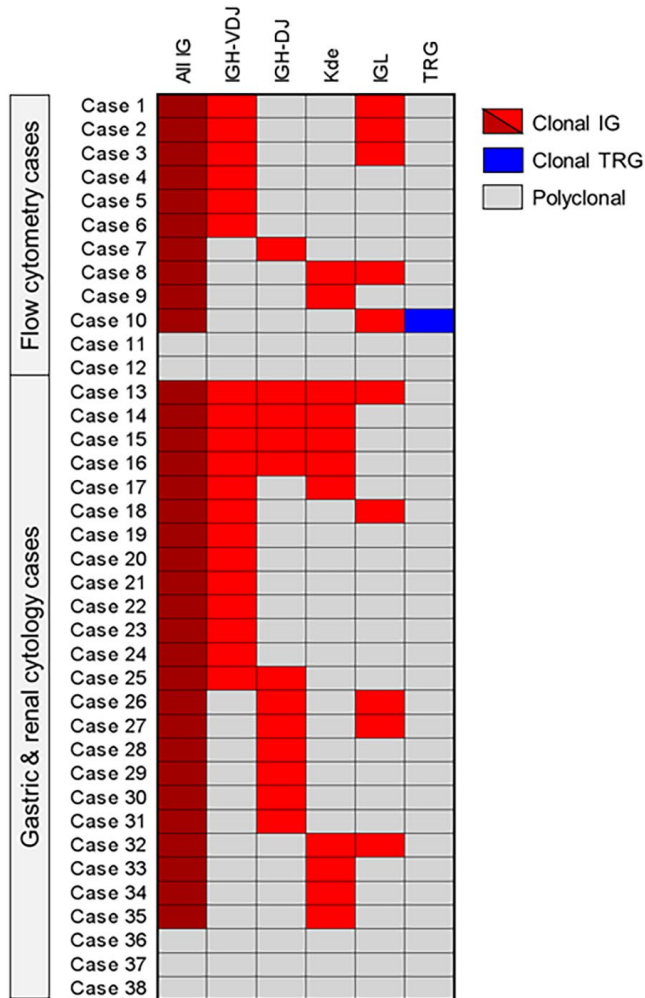


FIGURE 4 PCR for antigen receptor rearrangements (PARR) results for flow cytometrically confirmed B-cell lymphoma cases and cytologically confirmed gastric and renal lymphoma cases. Complete immunoglobulin heavy (IGH) chain variable (V)-diversity (D)-joining (J) (IGH-VDJ), incomplete immunoglobulin heavy chain D-J (IGH-DJ), kappa deleting element (Kde), immunoglobulin lambda (IGL) light chain, and T-cell receptor gamma (TRG) PARR results are shown for each of the flow cytometrically confirmed B-cell lymphoma cases ($n = 12$) and cytologically confirmed gastric and renal lymphoma cases of presumed B-cell origin ($n = 26$). The 'All IG' results column on the left indicates whether any of the immunoglobulin (IG) rearrangements (IGH-VDJ, IGH-DJ, Kde, IGL) were clonal in that case. Ten of twelve (83%) flow cytometrically confirmed cases and 23/26 (88%) cytologically confirmed gastric and renal cases had a clonal IG rearrangement. One of thirty-eight cases also had a clonal TRG rearrangement

aspirates were submitted to the CSU-Clinical Immunology laboratory for immunophenotyping by flow cytometry. All cases had $>50\%$ cells in the large-size gate, and $>50\%$ of cells in the large-size gate were $CD21^+$ and $CD5^-$, consistent with a B cell phenotype (Figure 3). Three of fifteen cases were excluded for insufficient target DNA. Results for the remaining twelve cases are reported. Cytologically, 11/12 cases had a definitive diagnosis of lymphoma, and 1/12 cases was diagnosed as possible lymphoma.

Twenty-seven cases of cytologically confirmed gastric ($n = 18$) and renal ($n = 9$) lymphoma were collected from June 13, 2014 to June 30, 2018. All cytology reports were reviewed, and when available, slides were reviewed by the authors (EDR and PRA). Cases had consistent cytomorphology, with intermediate to large-sized lymphocytes, with small to moderate amounts of basophilic cytoplasm, variably prominent nucleoli, and frequently few to several small punctate cytoplasmic vacuoles (Figure 3). One case was excluded for insufficient DNA, and results are reported for the remaining 26 cases ($n = 17$ gastric and nine renal cases).

T-cell leukemia cases were selected from peripheral blood samples submitted to the CSU-Clinical Immunology laboratory for immunophenotyping by flow cytometry between January 1, 2017 and July 12, 2018. Inclusion criteria included a lymphocyte count of $>60\,000$ lymphocytes/ μl on CBC where $>60\%$ of leukocytes were $CD21^- CD5^+$ T cells by flow cytometry. Fifty-five cases met inclusion criteria and had stored peripheral blood or flow cytometry cell pellets available for PARR. Thirty of these 55 cases were randomly selected for PARR analysis, and all 30 cases had sufficient target DNA for PARR amplification.

Eleven control cats were identified at necropsy that had no evidence of lymphoproliferative disease by histology or flow cytometry. Fresh mesenteric lymph node tissue was collected from all 11 cats. Peripheral blood was available from 10/11 of these cats, and CBC parameters were confirmed to be within normal limits. All samples had sufficient target DNA for PARR amplification.

3 | RESULTS

Twelve cases of flow cytometrically confirmed B-cell lymphoma were tested for clonality with the PARR assay. Signalment data and sampling sites are summarized in Table 2. By flow cytometry, the cases had 50%-92% of leukocytes in the large-size gate, and 55%-98% of cells in the large-size gate were $CD21^+$ B cells. Clonality analysis revealed that 10/12 (83%) cases had a clonal IG rearrangement, and the remaining 2/12 cases had polyclonal IG rearrangements (Figure 4). One case had a clonal TRG rearrangement; this case had cellular material from renal and ileum sites pooled for PARR. Comparing IG primer sets, 6/12 (50%) cases had clonal complete IGH-VDJ rearrangements, and three of these six cases had a concurrent clonal IGL rearrangement (Figures 4 and 5). Four of twelve (33%) cases had polyclonal IGH-VDJ rearrangements, but IG clonality was detected by clonal IGH-DJ, Kde, and/or IGL rearrangements.

Twenty-six samples of cytologically confirmed gastric ($n = 17$) and renal ($n = 9$) lymphoma, presumed to be of B-cell lineage due to their anatomic location and consistent cytomorphology (Figure 3), had clonality testing. Signalment data and sampling sites are summarized in Table 2. 23/26 (88%) cases had a clonal IG rearrangement, and the remaining 3/26 cases had polyclonal IG rearrangements (Figure 4). All 26 cases had polyclonal TRG rearrangements. 13/26 (50%) cases had clonal complete IGH-VDJ rearrangements, and seven of these 13 cases had a concurrent clonal rearrangement with another IG primer set: IGH-DJ, Kde, or IGL (Figures 4 and 5). Ten

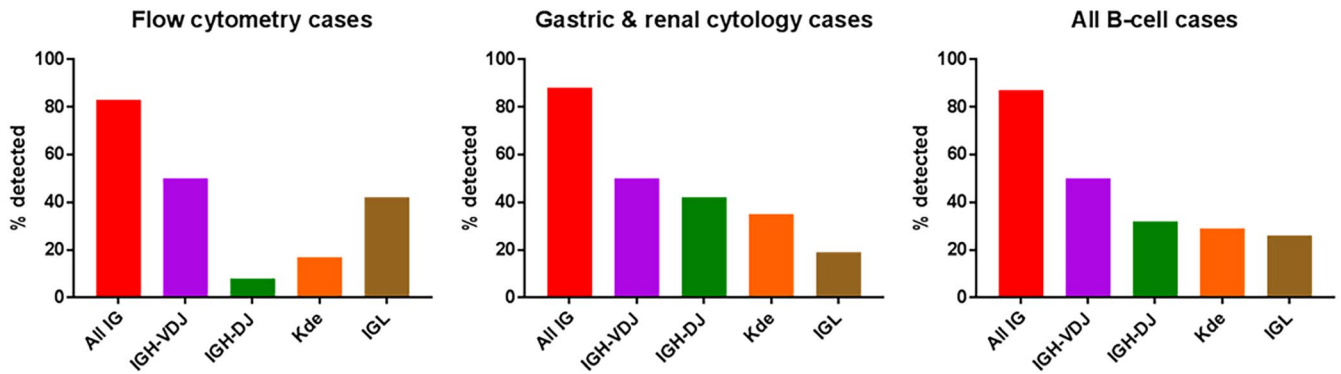


FIGURE 5 PCR for antigen receptor rearrangements (PARR) results for immunoglobulin (IG) gene rearrangements in flow cytometrically confirmed B-cell lymphoma cases and cytologically confirmed gastric and renal lymphoma cases. The percentage of cases with a clonal IG gene rearrangement is reported for each type of IG reaction. The red bar (all IG reactions) indicates the percentage of cases that had at least one clonal IG reaction when the data from each of the four IG reactions were combined for analysis. Results are shown for flow cytometrically confirmed B-cell lymphoma cases only ($n = 12$) (left), cytologically confirmed gastric and renal lymphoma cases of presumed B-cell origin only ($n = 26$) (center), and all B-cell lymphoma cases ($n = 38$) (right). Clonality was detected in 50% of all B-cell lymphoma cases with the IGH-VDJ reaction alone. Individual IGH-DJ, Kde, and IGL reactions detected between 26% and 32% of cases independently. When clonality results from all four of these IG reactions were combined, a clonal IG rearrangement was detected in 87% (33/38) of cases. Abbreviations: IGH-VDJ, complete immunoglobulin heavy chain variable (V)-diversity (D)-joining (J) gene rearrangement; IGH-DJ, incomplete immunoglobulin heavy chain diversity (D)-joining (J) gene rearrangement; Kde, kappa deleting element; IGL, immunoglobulin lambda

of twenty-six (38%) cases had polyclonal IGH-VDJ rearrangements, but IG clonality was detected by clonal IGH-DJ, Kde, and/or IGL rearrangements.

Thirty T-cell leukemia cases had clonality testing. The median age of patients was 11.6 years (IQR, 10.2-13.1 years; range, 3.4-16.4 years). The median lymphocyte count was 85 020 lymphs/ μL (IQR, 71 717-113 213 lymphs/ μL ; range, 61 400-374 100 lymphs/ μL). The percentage of CD5^+ T cells ranged from 60% to 96% of the total leukocytes, and CD21^+ B cells accounted for <7% of the total leukocytes. In CD4^+ T-cell leukemia cases ($n = 25$), <5% of the T cells were CD8^+ T cells. In $\text{CD4}^- \text{CD8}^-$ T-cell leukemia cases ($n = 5$), CD4^+ T cells and CD8^+ T cells accounted for <5% of all of the T cells. PARR revealed that 29/30 (97%) cases had a clonal TRG rearrangement (Figure 6). Clonal T-cell cases had between 1 and 8 clonal TRG peaks (mean, 3 peaks) when data from the TRG reactions using all four TRG primers were combined for analysis. All T-cell leukemia cases had polyclonal IG rearrangements with all four IG primer sets.

Eleven cats without lymphoproliferative disease were evaluated as negative controls. These cats were young adults (estimated ages, 1-5 years old), except for one 4-month-old kitten and one 10-year-old cat. Flow cytometry and histology performed on mesenteric lymph node samples showed no evidence of lymphoproliferative disease. In 10/11 cases, blood was available, and lymphoproliferative disease was not evident by flow cytometry, CBC, or blood smear review. In the 11 mesenteric lymph node samples and 10 blood samples from these cats, all IG rearrangements (using all 4 IG primer sets) and all TRG rearrangements were polyclonal (Figure 6).

When data from flow cytometrically confirmed B-cell lymphoma cases ($n = 12$) and cytologically confirmed gastric and renal lymphoma cases ($n = 26$) were combined for statistical analysis, the sensitivity of

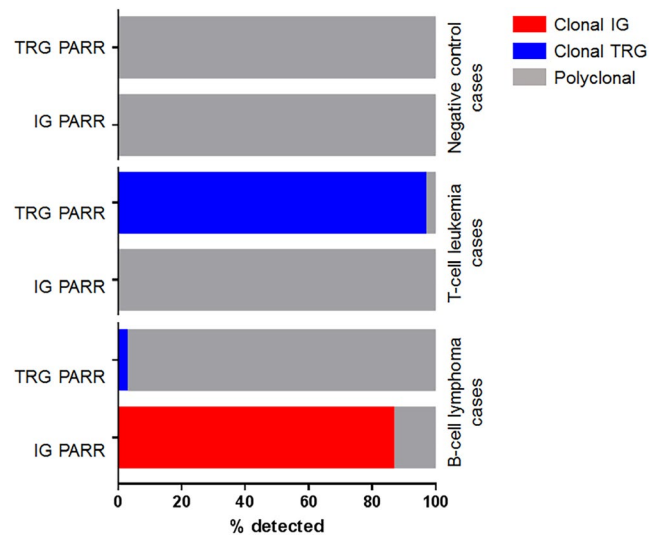


FIGURE 6 PCR for antigen receptor rearrangements (PARR) results for immunoglobulin (IG) gene rearrangements and T-cell receptor gamma (TRG) rearrangements in B-cell lymphoma cases, T-cell leukemia cases, and control cases without lymphoproliferative disease. The percentage of cases with a clonal IG rearrangement (red), clonal TRG rearrangement (blue), or polyclonal rearrangements (grey) is depicted within three cohorts of cases: B-cell cases (including data from both flow cytometrically confirmed and cytologically confirmed renal/gastric cases, $n = 38$), flow cytometrically confirmed T-cell leukemia cases ($n = 30$), and negative control cases with no evidence of lymphoproliferative disease ($n = 11$). Eighty-seven percent of B-cell cases had a clonal IG rearrangement when clonality results from all four IG reactions were combined for analysis. Ninety-seven percent of T-cell cases had a clonal TRG rearrangement. All negative control cases had polyclonal IG and TRG rearrangements

IG PARR to detect clonality in these presumed B-cell cases was 87% (33/38 cases), when using all four IG primer sets. The sensitivity of IGH-VDJ PARR alone to detect clonality in these cases was only 50% (19/38 cases). The sensitivity of TRG PARR to detect clonality in T-cell leukemia samples was 97% (29/30 cases). The specificity of both IG and TRG PARR in cats without lymphoproliferative disease was 100% ($n = 21$ samples from 11 cats). If we assume that T-cell leukemia cases had only T-cell neoplasia, and the B-cell cases only had B-cell neoplasia, then the overall specificity of IG PARR among the T-cell leukemia cases and negative control cases was 100% ($n = 41$), and the overall specificity of TRG PARR among the B-cell cases and negative control cases was 98% (48/49 cases).

Finally, nonspecific peaks can pose a challenge in interpreting PARR results and are well characterized in human clonality assays.³⁴ In the feline PARR assay described here, a consistent nonspecific TRG peak was detected in all cases with the TRGJ-r1 primer (Figure 7). This nonspecific peak is 232-233 nucleotides in length and outside the size range of TRG PCR products and is, therefore, easily detected as a spurious, nonclonal peak.

A TRG peak 78.5-78.7 nucleotides in length arising from the TRGJ-r2 primer was seen in a subset of cases (Figure 7). This peak was detected in 5/38 (13%) B-cell lymphoma cases, 2/30 (7%) T-cell leukemia cases, and a mesenteric lymph node from one of the negative control cases; however, the amplitude of the peak reached diagnostic criteria for clonality in only one case, which was a clonal T-cell leukemia case with other clonal TRG products. This peak is inconsistently detected and falls within the size range of TRG PCR products, making it challenging to determine whether the peak represents a true clone. To be conservative, in the rare cases where this product is of high amplitude, if the only discrete PCR product is the 78.5-78.7 nucleotide TRGJ-r2 peak, the result is not considered clonal.

Large-sized clonal PCR products are seen in IGH reactions when an IGHJ primer binds to an IGHJ gene downstream of the rearranged J gene. The large-sized product could be seen in addition to the primary clonal product, or, if an IGHJ primer does not anneal to the rearranged J gene, the large-sized product could be the only clonal product detected. In two B-cell cases, IGH-VDJ clonality was only detected by

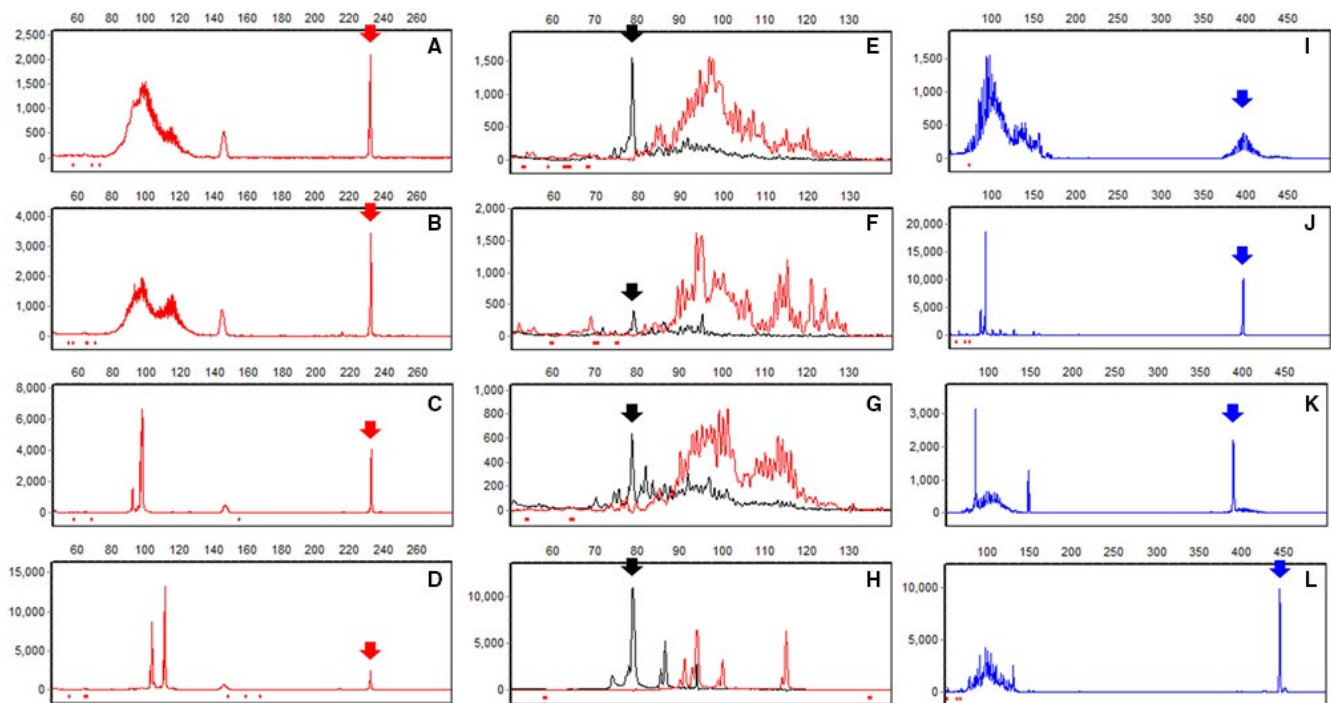


FIGURE 7 PCR for antigen receptor rearrangements (PARR) nonspecific peaks in T-cell receptor gamma (TRG) reactions (A-H) and large clonal PCR products in immunoglobulin heavy chain variable (V)-diversity (D)-joining (J) (IGH-VDJ) reactions (I-L). Left: A consistent nonspecific peak 232-233 nucleotides in length is seen in all TRG reactions, arising from the red PET-labeled TRGJ-r1 primer. Two polyclonal TRG cases (A and B) and two clonal TRG cases (C and D) are shown; each case has the nonspecific peak at varying amplitude. This artifact is outside the size range of TRG PCR products, and therefore, does not affect PARR interpretation. Center: A TRG peak 78.5-78.7 nucleotides in length arising from the black NED-labeled TRGJ-r2 primer can be seen in a subset of cases, including B-cell lymphoma cases that otherwise have polyclonal TRG rearrangements (E-G), and rare T-cell leukemia cases that have additional clonal TRG rearrangements (H). This product is usually of low amplitude (E-G), but can reach an amplitude (>3000) consistent with a clonal product (H). This product falls within the size range of black TRG PCR products and complicates the diagnosis. Right: Large-sized products are seen in the IGH-VDJ reaction when the IGHJ primer anneals to a downstream IGHJ gene. In a polyclonal case (I), the typical IGH-VDJ rearrangements form a Gaussian distribution in the 70-170 nucleotide size range, and the large-sized products form a second Gaussian distribution of lower amplitude in the 370-470 nucleotide size range. Two clonal B-cell cases (J and K) have a typical clonal IGH-VDJ rearrangement and a clonal large-sized product. One B-cell case (L) with only a clonal large-sized product is shown

a large-sized product (Figure 7). The size of the large IGH-VDJ clonal PCR products with downstream IGJ genes can be predicted based on the known number of nucleotides between each of the IGJ genes.

4 | DISCUSSION

The goal of this study was to evaluate the sensitivity and specificity of our currently configured PARR assay for detecting IG and TCR rearrangements in feline lymphoproliferative disorders. In this study, we used ideal sample types to test the assay under optimal conditions. This was done to help identify B-cell lymphomas as well as avoid cases with ambiguous diagnoses of lymphoproliferative disease. Small cell gastrointestinal T-cell lymphomas, in particular, can be challenging to diagnose definitively, so T-cell leukemias were selected to represent feline T-cell neoplasms.^{5,6} Samples were of high cellularity, and neoplastic lymphocytes comprised the majority of the lymphocyte population by cytology and/or flow cytometry. Under these conditions, the IG PARR assay containing four IG primer sets had a sensitivity of 87% and an overall specificity of 98%. The TRG PARR assay had a sensitivity of 97% and specificity of 100%. These sensitivity and specificity values apply only to these primers when used under these cycling conditions with these fragment analysis methods. This is the first step in evaluating the clinical utility of the primers developed here. With knowledge of the sensitivity and specificity of the assay under ideal conditions, we can now assess the PARR assay in circumstances where the diagnosis of lymphoma is uncertain. Those types of samples are often challenging to assess for diagnostic accuracy because a definitive diagnosis can be difficult to achieve, even with histopathology as a gold standard. Sabattini et al compared diagnostic methods for differentiating inflammatory bowel disease from lymphoma in feline duodenal samples, finding that clonality had the highest prognostic value and histology incorrectly diagnosed a number of lymphomas as inflammatory.⁵ Notwithstanding the challenges of identifying a gold standard method, feline samples composed of small lymphocytes or mixed lymphoid populations, especially from the gastrointestinal tract, represent the most common samples submitted for clonality testing, and the second phase of this study assesses the diagnostic accuracy of this PARR assay in those samples.

A central finding of this study was that the sensitivity of IG PARR increased significantly when we assessed other IG rearrangements beyond complete IGH-VDJ rearrangements. Incomplete IGH-DJ rearrangements are targeted in human clonality testing and are less affected by somatic hypermutation.³⁴ We detected clonal incomplete IGH-DJ rearrangements in 32% (12/38) of B-cell lymphoma cases. Kde clonality testing in human medicine increases the number of B-cell neoplasms detected because virtually all lambda-expressing B-cell tumors and a subset of kappa-expressing tumors have Kde rearrangements, and Kde rearrangements show no or little somatic hypermutation.³⁴ In this study, a clonal Kde rearrangement was detected in 29% (11/38) of feline B-cell cases. Additionally, we designed an IGL PARR assay targeting the IGLV1 subgroup genes. Lu et al characterized the feline IGL genes and reported their use.¹⁵ Among 49 clone sequences from two cats, they mapped 36/49 (73%) sequences to the IGLV1 subgroup.

Given this usage in healthy cats, we hypothesized we would detect the majority of IGL rearrangements in B-cell neoplasms with IGLV1 primers alone, but we only detected clonal IGL rearrangements in 26% (10/38) of the B-cell cases. This Kde assay only detected rearrangements where the Kde rearranged with the IGKJ-IGKC intron, but the Kde could also rearrange with IGKV gene segments.³⁵ Designing forward primers to IGKV genes might increase the number of Kde rearrangements detected. Additionally, we are designing IGL PARR primers to target other IGLV subgroups, which could increase the sensitivity of IGL PARR. The traditionally employed IGH-VDJ assay only detected 50% of the B-cell neoplasms in this study, which is within the range detected by some of the other publications assaying this region.^{22,23,26} This could be partly due to the types of samples selected; for example, if the B-cell neoplasms sampled have a high degree of somatic hypermutation, primer annealing could be compromised. In human medicine, certain subtypes, including diffuse large B-cell lymphomas, usually have large numbers of somatic mutations.³⁴ Given the moderate sensitivity of IGH-VDJ PARR alone, we now combine all four IG primer sets for every feline PARR assay, to increase the sensitivity for detecting B-cell neoplasia.

In this study, the PARR assay had high sensitivity for detecting neoplasia as well as identifying cell lineages. In 30 T-cell leukemia cases, PARR appropriately detected a clonal TRG rearrangement in all 29 cases that were identified as neoplastic by PARR, and no clonal IG rearrangements were identified. The T-cell lineage of these cases was determined using flow cytometry as a gold standard. It was more challenging to definitively identify B-cell lymphoma cases for clonality testing. B-cell leukemia is rare in cats,³⁶ so we were unable to collect flow cytometrically confirmed B-cell leukemia cases, but rather searched for B-cell lymphoma cases from any site that were definitively diagnosed by flow cytometry. Because cats can have expansions of small-sized B cells in reactive processes,³⁷ we restricted our criteria to cases with expanded large-sized B cells. These criteria yielded a small number of cases, so we sought additional cases by identifying cytologically confirmed cases from two sites most commonly associated with B-cell lineage lymphoma: stomach and kidney.^{22,30-32} Among these cytologically confirmed gastric and renal lymphoma cases, all cases that were identified as neoplastic by PARR had a clonal IG rearrangement and polyclonal TRG rearrangements, consistent with the B-cell lineage. Of the flow cytometrically confirmed B-cell lymphoma cases, one case had both clonal IG and TRG rearrangements, while all other cases had polyclonal TRG rearrangements. This one B-cell lymphoma case had cytologically prepared slides from the kidney and ileum combined for PARR analysis, raising the possibility that the patient had two tumors, a renal B-cell lymphoma and intestinal T-cell lymphoma.

Tumors arising from precursor cells, including a subset of acute myeloid leukemias and precursor B-cell acute lymphoblastic leukemias,^{34,38} can have clonal rearrangements that are not representative of the cell of origin, but lineage infidelity is rare in neoplasms arising from more mature cells.³⁹ Cross-lineage clonal rearrangements have been described in feline B-cell and T-cell lymphomas.^{18,26,28,40} However, it is possible that some of these cases had concurrent B-cell and T-cell neoplasms, as cats could have had two neoplasms within the GI tract.²² Another possibility is that there are invariant T-cell

rearrangements or TRG rearrangements with limited to no junctional diversity, which generate a product that appears clonal. We hypothesize that the 78.5-78.7 nucleotide TRG peak that appeared at a low amplitude in B-cell neoplasms and one negative control case represents a population of gamma-delta T cells with an invariant TCR rearrangement or rearrangements within a TRG cassette that has very limited junctional diversity. We suspect other laboratories might or might not detect this product depending on the primers used. Weiss et al¹⁸ also described feline TRG rearrangements that seemed equivalent to canonical TRG proteins, hypothesized to arise early in fetal development and have no junctional diversity. Future directions include cloning and sequencing of this rearrangement. The dilemma faced with this PCR product highlights the utility of both fragment analysis technology and establishing objective criteria to diagnose clonal products. Fragment analysis provides fragment length to a single nucleotide resolution, which allowed for the identification of identically sized products across multiple samples, raising suspicion that this was not a true clonal product. Also, the product amplitude was never 3× the base in B-cell or negative control cases, so it did not reach objective criteria for clonality. Without these criteria, this product could have been identified as a cross-lineage rearrangement.

In conclusion, the PARR assay described in this study was useful in assessing clonality in feline lymphoid tumors. This assay was developed for fresh tissues and air-dried cytologic preparations and had a high sensitivity for detecting clonality in the optimal sample types tested. There were no falsely clonal results in control cats without lymphoproliferative disease, and the lineage identified as neoplastic by PARR was as expected for nearly all cases with a clonal result, indicating high specificity. The sensitivity of IG PARR was greatly improved by examining incomplete IGH-DJ and IG light chain rearrangements, in addition to the commonly examined complete IGH-VDJ rearrangements.

ACKNOWLEDGMENTS

The authors thank Dr Marie-Paule Lefranc and the international ImMunoGeneTics information system for their invaluable expertise and assistance.

DISCLOSURE

The authors have indicated that they have no affiliations or financial involvement with any organization or entity with a financial interest in, or in financial competition with, the subject matter or materials discussed in this article.

ORCID

Emily D. Rout  <https://orcid.org/0000-0003-1435-8532>

REFERENCES

1. Louwerens M, London CA, Pedersen NC, Lyons LA. Feline lymphoma in the post-feline leukemia virus era. *J Vet Intern Med.* 2005;19:329-335.
2. Sato H, Fujino Y, Chino J, et al. Prognostic analyses on anatomical and morphological classification of feline lymphoma. *J Vet Med Sci.* 2014;76:807-811.
3. Amores-Fuster I, Cripps P, Graham P, Marrington AM, Blackwood L. The diagnostic utility of lymph node cytology samples in dogs and cats. *J Small Anim Pract.* 2015;56:125-129.
4. Ku CK, Kass PH, Christopher MM. Cytologic-histologic concordance in the diagnosis of neoplasia in canine and feline lymph nodes: a retrospective study of 367 cases. *Vet Comp Oncol.* 2017;15:1206-1217.
5. Sabattini S, Bottero E, Turba ME, Vicchi F, Bo S, Bettini G. Differentiating feline inflammatory bowel disease from alimentary lymphoma in duodenal endoscopic biopsies. *J Small Anim Pract.* 2016;57:396-401.
6. Kiupel M, Smedley RC, Pfent C, et al. Diagnostic algorithm to differentiate lymphoma from inflammation in feline small intestinal biopsy samples. *Vet Pathol.* 2011;48:212-222.
7. Waly NE, Gruffydd-Jones TJ, Stokes CR, Day MJ. Immunohistochemical diagnosis of alimentary lymphomas and severe intestinal inflammation in cats. *J Comp Pathol.* 2005;133:253-260.
8. Briscoe KA, Krockenberger M, Beatty JA, et al. Histopathological and immunohistochemical evaluation of 53 cases of feline lymphoplasmacytic enteritis and low-grade alimentary lymphoma. *J Comp Pathol.* 2011;145:187-198.
9. Moore PF, Woo JC, Vernau W, Kosten S, Graham PS. Characterization of feline T cell receptor gamma (TCRG) variable region genes for the molecular diagnosis of feline intestinal T cell lymphoma. *Vet Immunol Immunopathol.* 2005;106:167-178.
10. Burnett RC, Vernau W, Modiano JF, Olver CS, Moore PF, Avery AC. Diagnosis of canine lymphoid neoplasia using clonal rearrangements of antigen receptor genes. *Vet Pathol.* 2003;40:32-41.
11. Langerak AW, Groenen P, Brüggemann M, et al. EuroClonality/BIOMED-2 guidelines for interpretation and reporting of Ig/TCR clonality testing in suspected lymphoproliferations. *Leukemia.* 2012;26:2159-2171.
12. Keller SM, Moore PF. Rearrangement patterns of the canine TCR γ locus in a distinct group of T cell lymphomas. *Vet Immunol Immunopathol.* 2012;145:350-361.
13. Henrich M, Hecht W, Weiss AT, Reinacher M. A new subgroup of immunoglobulin heavy chain variable region genes for the assessment of clonality in feline B-cell lymphomas. *Vet Immunol Immunopathol.* 2009;130:59-69.
14. Das S, Nozawa M, Klein J, Nei M. Evolutionary dynamics of the immunoglobulin heavy chain variable region genes in vertebrates. *Immunogenetics.* 2008;60:47-55.
15. Lu Z, Tallmadge RL, Callaway HM, Felipe M, Parker J. Sequence analysis of feline immunoglobulin mRNAs and the development of a feline monoclonal antibody specific to feline panleukopenia virus. *Sci Rep.* 2017;7:1-15.
16. Weiss A, Hecht W, Henrich M, Reinacher M. Characterization of C-, J- and V-region-genes of the feline T-cell receptor γ . *Vet Immunol Immunopathol.* 2008;124:63-74.
17. Weiss A, Hecht W, Reinacher M. Feline T-cell receptor V- and J-region sequences retrieved from the trace archive and from transcriptome analysis of cats. *Vet Med Int.* 2010;2010:1-7.
18. Weiss A, Klopffleisch R, Gruber A. T-cell receptor γ chain variable and joining region genes of subgroup 1 are clonally rearranged in feline B- and T-cell lymphoma. *J Comp Pathol.* 2011;144:123-134.
19. Mochizuki H, Nakamura K, Sato H, et al. Multiplex PCR and Genescan analysis to detect immunoglobulin heavy chain gene rearrangement in feline B-cell neoplasms. *Vet Immunol Immunopathol.* 2011;143:38-45.
20. Mochizuki H, Nakamura K, Sato H, et al. GeneScan analysis to detect clonality of T-cell receptor γ gene rearrangement in feline lymphoid neoplasms. *Vet Immunol Immunopathol.* 2012;145:402-409.

21. Werner JA, Woo JC, Vernau W, et al. Characterization of feline immunoglobulin heavy chain variable region genes for the molecular diagnosis of B-cell neoplasia. *Vet Pathol.* 2005;42:596-607.
22. Moore PF, Rodriguez-Bertos A, Kass PH. Feline gastrointestinal lymphoma: mucosal architecture, immunophenotype, and molecular clonality. *Vet Pathol.* 2012;49:658-668.
23. Henrich M, Scheffold S, Hecht W, Reinacher M. High resolution melting analysis (HRM) for the assessment of clonality in feline B-cell lymphomas. *Vet Immunol Immunopathol.* 2018;200:59-68.
24. Steiniger S, Glanville J, Harris DW, Wilson TL, Ippolito GC, Dunham SA. Comparative analysis of the feline immunoglobulin repertoire. *Biologicals.* 2017;46:81-87.
25. Brüggemann M, White H, Gaulard P, et al. Powerful strategy for polymerase chain reaction-based clonality assessment in T-cell malignancies report of the BIOMED-2 Concerted Action BHM4 CT98-3936. *Leukemia.* 2007;21:215-221.
26. Hammer SE, Groiss S, Fuchs-Baumgartinger A, et al. Characterization of a PCR-based lymphocyte clonality assay as a complementary tool for the diagnosis of feline lymphoma. *Vet Comp Oncol.* 2017;15:1354-1369.
27. Gress V, Wolfesberger B, Fuchs-Baumgartinger A, et al. Characterization of the T-cell receptor gamma chain gene rearrangements as an adjunct tool in the diagnosis of T-cell lymphomas in the gastrointestinal tract of cats. *Res Vet Sci.* 2016;107:261-266.
28. Sato H, Fujino Y, Uchida K, Ohno K, Nakayama H, Tsujimoto H. Comparison between immunohistochemistry and genetic clonality analysis for cellular lineage determination in feline lymphomas. *J Vet Med Sci.* 2011;73:945-947.
29. Arun SS, Breuer W, Hermanns W. Immunohistochemical examination of light-chain expression (lambda/kappa ratio) in canine, feline, equine, bovine and porcine plasma cells. *Zentralbl Veterinarmed A.* 1996;43:573-576.
30. Gabor LJ, Canfield PJ, Malik R. Immunophenotypic and histological characterisation of 109 cases of feline lymphosarcoma. *Aust Vet J.* 1999;77:436-441.
31. Vail DM, Moore AS, Ogilvie GK, Volk LM. Feline lymphoma (145 cases): proliferation indices, cluster of differentiation 3 immunoreactivity, and their association with prognosis in 90 cats. *J Vet Intern Med.* 1998;12:349-354.
32. Pohlman LM, Higginbotham ML, Welles EG, Johnson CM. Immunophenotypic and histologic classification of 50 cases of feline gastrointestinal lymphoma. *Vet Pathol.* 2009;46:259-268.
33. Lefranc M-P, Giudicelli V, Duroux P, et al. IMGT, the international ImMunoGeneTics information system 25 years on. *Nucleic Acids Res.* 2015;43:D413-D422.
34. van Dongen J, Langerak AW, Brüggemann M, et al. Design and standardization of PCR primers and protocols for detection of clonal immunoglobulin and T-cell receptor gene recombinations in suspect lymphoproliferations: report of the BIOMED-2 Concerted Action BMH4-CT98-3936. *Leukemia.* 2003;17:2257-2317.
35. Beishuizen A, de Bruijn M, Pongers-Willems MJ, et al. Heterogeneity in junctional regions of immunoglobulin kappa deleting element rearrangements in B cell leukemias: a new molecular target for detection of minimal residual disease. *Leukemia.* 1997;11:2200-2207.
36. Campbell MW, Hess PR, Williams LE. Chronic lymphocytic leukaemia in the cat: 18 cases (2000-2010). *Vet Comp Oncol.* 2013;11:256-264.
37. Weiss DJ. Differentiating benign and malignant causes of lymphocytosis in feline bone marrow. *J Vet Intern Med.* 2005;19:855-859.
38. Stokol T, Nickerson GA, Shuman M, Belcher N. Dogs with acute myeloid leukemia have clonal rearrangements in T and B cell receptors. *Front Vet Sci.* 2017;4:76. <https://doi.org/10.3389/fvets.2017.00076>.
39. Medeiros LJ, Carr J. Overview of the role of molecular methods in the diagnosis of malignant lymphomas. *Arch Pathol Lab Med.* 1999;123:1189-1207.
40. Andrews C, Operacz M, Maes R, Kiupel M. cross lineage rearrangement in feline enteropathy-associated T-cell lymphoma. *Vet Pathol.* 2016;53:559-562.

SUPPORTING INFORMATION

Additional supporting information may be found online in the Supporting Information section at the end of the article.

How to cite this article: Rout ED, Burnett RC, Yoshimoto JA, Avery PR, Avery AC. Assessment of immunoglobulin heavy chain, immunoglobulin light chain, and T-cell receptor clonality testing in the diagnosis of feline lymphoid neoplasia. *Vet Clin Pathol.* 2019;48(Suppl. 1):45-58. <https://doi.org/10.1111/vcp.12767>